ISABE-2015-20097

PREPARING FOR PROOF-OF-CONCEPT OF A NOVEL PROPELLER FOR OPEN ROTOR ENGINES

Richard Avellán
GKN Aerospace Sweden
SE-46181 Trollhättan, Sweden

Alexandre Capitao Patrao
Chalmers University of Technology
SE-41296 Gothenburg, Sweden

Anders Lundbladh
GKN Aerospace Sweden
SE-46181 Trollhättan, Sweden

Tomas Grönstedt
Chalmers University of Technology
SE-41296 Gothenburg, Sweden

Abstract

This article describes the development of a novel high-speed propeller concept. Large-scale propeller tests are extremely expensive and thus not appropriate at early R&D development phases. A convenient approach is to use computational methods validated by small-scale tests with propellers manufactured from low-cost materials and rapid manufacturing methods. The present paper is describing this cross validation work explaining differences between numerics and experiments. Preferred materials and manufacturing methods for high-speed future wind tunnel tests are discussed. We also discuss the progress of development of the aerodynamic design of the concept propeller.

Nomenclature

AM	Additive Manufacturing
ATP	Advanced Turboprop Project
C_T	Thrust coefficient, $T/\rho N^2D^4$
C_P	Power coefficient, $P/\rho N^3D^5$
D	Propeller diameter
EBM	Electron Beam Melting
HTR	Hub-to-Tip radius ratio
J	Advance ratio, V/ND
M	Mach number
MMP	Micro Machining Process
N	Rotational speed
P	Power
ρ	Air density
R_a	Arithmetic average roughness
R&D	Research and development
SLA	Stereolithography
SLM	Selective Laser Melting
T	Net thrust
V	Free-stream velocity

Introduction

One of the greatest potential advances in aircraft fuel consumption and operating cost within the next 20 years is the introduction of engines with high speed propellers, e.g. open rotor fans. In 2009, a novel propeller concept intended for high speed flight, the Boxprop, was presented by the authors[1,2], see Figure 1. The basic idea is to utilize pairwise joined blades to give a number of advantages compared to the conventional propeller. Several hypotheses regarding the potential benefits of the propeller were presented, including improved aerodynamics and reduced noise.

Figure 1 - Prototype of wind tunnel test Boxprop with adjustable pitch blades made by Selective Laser Melting, AlSi10Mg. 150 mm diameter.

Reinventing the high-speed propeller

The energy crisis that the western world experienced in the 1970s affected people's lives in many ways. One example was when the U.S. airline industry furloughed some 25,000 people during 1974 and Pan American, the largest operator in the U.S. at that time, stopped operating in 12 cities during the same year[3]. But it also resulted in a change in focus of the aeronautical research in the western world. The old glamorous aerospace research paradigm of going faster, higher, farther shifted focus to perhaps more essential goals such as lower fuel consumption and energy conservation.

On a direct request from the U.S. congress NASA initiated a series of R&T programs with the overall objective of a 50% reduction in fuel consumption for commercial and military aviation in the U.S. Some of the research programs were focusing on aircraft technologies, e.g. composite structures, laminar flow control, winglets while others focused on technologies for more efficient engines. The engine R&T program with the greatest potential for fuel savings was the advanced turboprop project (ATP) which resulted in successful demo flights of both single- and counter-rotating high speed propellers. General Electric and NASA developed the unducted fan (UDF) gearless counter-rotating open rotor engine, Pratt & Whitney and Allison demonstrated the geared counter-rotating 578-DX propfan, addition-ally an advanced single-rotating propfan was demonstrated by NASA and Hamilton Standard. The key to success for all of these demonstrations was the development of the high-speed propellers that needed to achieve high efficiencies at the same flight speeds as jet-driven aircraft. Propellers operate in the free-stream air without a nacelle inlet section that decelerates the flow which required the development of very thin and highly swept carbon fiber composite propeller blades to suppress the compressibility losses that otherwise restricts conventional propellers to lower flight speeds than jets. Several advanced propeller concepts were also proposed during the ATP program of which very few were tested.

Two interesting concepts that were tested was the single-rotating propeller with a swirl-recovery vane and a counter-rotating concept with a forward-swept front rotor and an aft swept rear rotor[4], see Figure 2. The latter concept is interesting because it reflects one of unique features of the Boxprop concept, the forward swept front rotor. The motivation for introducing a forward swept front rotor was to reduce the interaction noise by increasing the blade tip separation of the front and aft rotor. However, due to aeromechanical issues with the front rotor that could not be overcome with the design tools and material data bases available at that point in time, the test campaign ended without any successful test data recorded at the design point so no conclusions concerning this idea could be drawn.

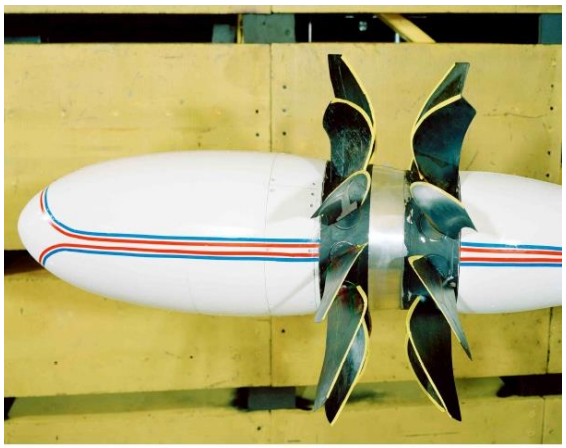

Figure 2 - The advanced forward-aft swept counter-rotating propeller concept tested by NASA during the final stages of the ATP program. Adapted from Van Zante[4].

In recent years the interest for high-speed propellers and open rotor engines has been renewed and in Europe the Clean Sky program is aiming towards a flight demonstration of the open rotor engine around 2019[5]. Quite recently in the U.S., GE, NASA and FAA cooperated to develop a new generation of high-speed blades, starting from the work done in the 1970s and 1980s[4].

Preparing for proof-of-concept

At low TRLs and before entering the product development phase, new concepts must be proofed using limited resources. Small-scale testing is a necessity in keeping the costs at reasonable levels in the early phases of product development. For claiming the Boxprop to have reached TRL 3 and for motivating further investment into this research, the propeller must function as intended and not being noticeably worse in any respect. Aerodynamic performance is identified as one of the potential benefits of the Boxprop and much of the work in the initial development phase is focused on validation of this concept through analysis and experiments on the laboratory scale[6].

More specifically, the purpose of the present work was to gain knowledge concerning small-scale propeller testing and to explain and quantify the differences between the results from the analytical work and experiments presented in the previous work[1].

Material selection and manufacturing of small scale propellers

For aerospace applications, specific material properties are of great importance since low weight is necessary for minimizing fuel burn. Early propellers were successfully manufactured from different types of laminated wood. Wood is a natural composite material that is strong in the grain direction and easily manufactured and formed to the desired shape. Compared to metals and fiber reinforced composites it can also be considered a low-cost material. Perhaps the most prominent example of the use of wood in aerospace applications is the Hughes aircraft H-4 Hercules, widely known as the "Spruce goose". This magnificent vehicle, which was perhaps more of a flying boat than an aircraft, was entirely manufactured from laminated wood and as a matter of fact it was mostly birch laminate and not spruce as the name implies[7]. Mahogany and walnut are other examples of wood materials used for early propeller designs. When aluminum alloy became cost competitive it became the most common material of choice for propellers in period after the First World War.

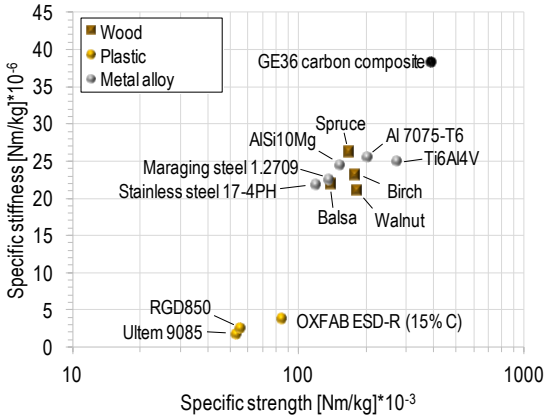

Figure 3 - Specific stiffness and strength of different materials considered for the manufacturing of propeller prototypes used in this work. The mechanical properties of the wood presented in this figure are obtained from testing of clear and straight-grained pieces of wood[8,9]. All the metal alloy data points represent "as-built" condition from the SLM process – except for the aircraft grade aluminum 7075-T6.

Today, wooden propellers are mostly used for low power applications. In Figure 3 the specific strength and stiffness of different materials relevant for this study are shown. It is obvious that carbon fiber

composite materials, for which the fiber orientation can be controlled, have good specific properties and are the preferred choice for future production propellers.

To date, the testing has been successful through the use of plastic propellers (Verogrey RGD850 and RGD525 photopolymers) manufactured from the PolyJet method which is an evolvement of the SLA process. These test used a non-scale blade thickness of about 8% profile at the tip and increasing towards the root. For 150 mm propellers this corresponded to a tip maximum thickness of 1.1 mm, with leading and trailing edge about half of this. The tests have been performed with blade tip speeds up to 210 m/s representative for full scale operation of a future counter rotating propeller.

Examination of test results and FE-modeling indicated that at high speed blade untwist significantly affected the experimental data. Accordingly the most accurate validation accounted for below was performed at 102 m/s tip speed, for which the maximum change of airfoil pitch angle was calculated to be 1.4 degrees.

For accurate testing at full rotational speed and also allowing for thinner blades necessary for cruise operating conditions, higher strength and stiffness materials such as metal or carbon fibre composites are needed. An interesting development for this research is a new carbon filled thermoplastic material for rapid prototyping was introduced by Oxford Performance Materials[10], OXFAB® ESD-R. A significant increase of strength and stiffness over non-reinforced 3D printing plastics has been demonstrated.

As a step towards propeller testing at higher speed conditions, a student project was initiated in cooperation between GKN and Chalmers University of Technology during spring semester 2014 with the objective of a recommended manufacturing method and material selection for small-scale propellers with complex blade shapes[10]. Several manufacturing methods and materials were investigated including multiaxis milling, EBM and SLM (Figure 4 - Figure 6). The surface roughness requirement was set to 1.1 µm Ra in the flow direction for achieving hydrodynamically smooth blade surfaces at high speed.

Figure 4 - 50 mm prototype blades manufactured from 1): multi-axis milling/Aluminum/thin profile, 2): SLM/ Aluminum/thin profile, 3): SLM/Titanium 4: SLM/Aluminum.

Several suppliers were asked to machine a test blade with a tip thickness representative of a production propeller which was set as 2% max profile thickness, or 0.26 mm for a 150 mm diameter propeller (thin profile in Figure 4). Although work holding to avoid chatter during milling is a significant challenge, IVG Engineering AB accepted and delivered a blade of acceptable quality. The relatively long machine preparation time drove the cost of one blade to about 5 times the cost of a complete fixed pitch PolyJet propeller, but this is expected to decrease somewhat as more blades are made. However, the milled blades did meet the smooth surface requirement and would not require any further polishing. For

comparison thin profile blades made by SLM had holes and were unusable.

The additive manufacturing processes investigated, i.e. EBM and SLM, did have a shorter preparation time so the price for a small prototype batch size was 1/8 of the price for the milled blades. One drawback with the AM processes studied here, is the quite rough surfaces, and a polishing method preserving the design geometry would be needed to meet the surface roughness requirement. Several possible after treatment methods were proposed including MMP finishing[12] and abrasive flow machining[13] (AFM).

Figure 5 - Close-up of propeller manufactured from EBM/Titanium. 120 mm diameter.

Figure 6 - Close-up of the propeller blade manufactured from SLM/Aluminum.

Although the AM manufactured blades did show lower unit cost one must consider the additional cost of polishing the blades with advanced after treatment methods together with the additional process validation needed since both MMP and AFM are subtractive methods, i.e. material is removed from the blades, and it is possible that material offsets are needed in the CAD blade model to compensate for this effect.

Concepts for an adjustable pitch mechanism

In order to derive the propeller off-design performance maps from the wind tunnel tests, the advance ratio and the blade angles must be varied. The advance ratio is varied by altering the tunnel wind speed and/or the rotational speed of the propeller. To capture the performance impact of the blade angle variation either a set of different propellers can be manufactured, each with a unique pitch angle, or a mechanism to adjust the pitch angle before start of each test run must be implemented. The Chalmers student team investigated several possible ways of solving this challenge within a limited budget. The final proposed concept is shown in Figure 1 and Figure 7. M5 high strength bolts attached the blades to the hub which is reinforced with steel thread inserts. The blade angles can be adjusted individually before each test run using the graded scale that is shown in Figure 7. The highest stress occurs in the bolt during design rotational speed of 26,000 rpm. By numerical analyses it was shown that, for the aluminum blades, the safety factor for the blade bolt and hub will be greater than two for all operating conditions, which is necessary to fulfill the rig safety requirements. A rig containment case will still be required.

Figure 7 - Final propeller concept with adjustable pitch angles. SLM manufactured aluminum blades with a machined aluminum hub.

Surface roughness – measurements

To determine whether it would be worth the effort of achieving smoother surfaces of the model propellers, one 150 mm RGD850 propeller manufactured from the PolyJet process was measured with a Somicronic Surfascan 3CS profilometer. Four strips at roughly R/R_{tip} = 0.8 and 9.7 mm of length in the streamwise direction were measured and the form and waves longer than 2.5 mm were filtered out.
The measured surface roughness was R_a 4.3 to 8.2 µm, with the higher values on the concave pressure sides. From the data the k_{rms} roughness was found to be 5.3 to 9.8 µm, with skewness in the range -0.43 to -0.06. Using the correlation by Flack and Schulz[14] the sand grain roughness was calculated to be an average of 24 µm. By weighting the suction side higher to approximately account for the increased skin friction on this side the weighted average sand grain sand grain roughness was found to be 21 µm. For the 13000 RPM small scale propeller the skin friction velocity is estimated at 5.4 m/s and the viscous length scale at 2.8 µm. This gives a roughness Reynolds number, k_s^+, of 7.5 which is in the transition flow regime and also fairly close to the limit for hydraulical smoothness ($k_s^+ < 5$). The expected increase of skin friction for a flat plate under these conditions is on the order of 10%[15]. A better quantification of the influence of roughness was derived through CFD.

Geometry validation of manufactured propellers

To quantify the geometric deviation between the as built propellers with the nominal model one of the propellers manufactured from PolyJet/RGD850 was measured with an ATOS core 300 optical measurement machine. The results are shown in Figure 8 indicating deviations of less than 0.25 mm except in the bend in the blade tip region were the individual blades are joined. This corresponds to below 1 degree blade angle and was not deemed significant for the testing.

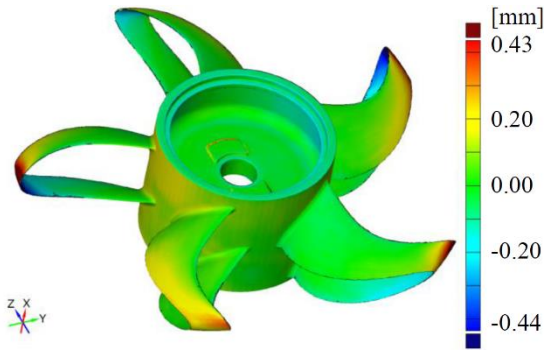

Figure 8 - GPX313 Boxprop with 150 mm diameter. Deviation of the manufactured propeller from the designed geometry.

Experimental aerodynamics

Tests were performed in the Chalmers low-speed wind tunnel. Air velocities between 0-60 m/s can be obtained in the 3 m long test section with an octagonal cross section 1.8×1.25 m. The test rig for counter-rotating propellers was designed and built during 2013, see the master's thesis report by Olofsson and Petterson[16]. For single rotation tests the rear propeller motor is replaced by a dummy cylinder, see Figure 9. Analysis and tests have shown that

measurement errors are within 2% in propeller thrust coefficient, C_T, and power coefficient, C_P.

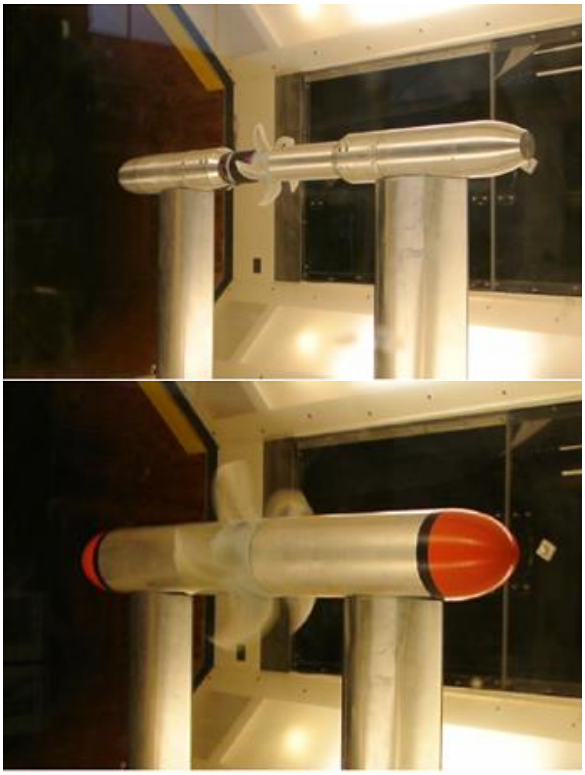

Figure 9 - The GPX313 propeller during the 2015 test campaign in the Chalmers low-speed wind tunnel, flow from left. Top: 150 mm diameter propeller. Bottom: 300 mm diameter propeller.

Low-speed conditions

In this paper, low speed refers to ISA, Sea level conditions with advance ratios present during take-off, and in particular the advance ratios between 0.15 and 0.92, which are achievable in the Chalmers wind tunnel at medium rotational tip speed (102 m/s).

The geometry used is the GPX313 propeller[1], seen in Figure 9. It has a diameter of 150 mm and consists of five tip-joined box-blades with an activity factor of 1800. This blade has been tested and analyzed numerically.

Computational aerodynamics

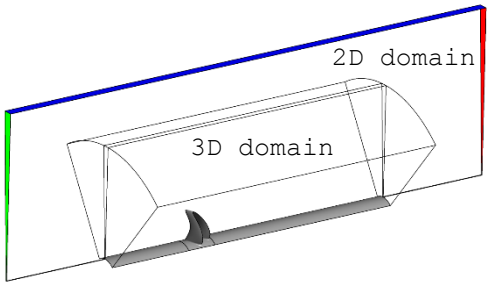

Figure 10 - Fluid domains and blade position. Inlet (green), opening (blue), outlet (red), and propeller/hub (grey). Flow from left.

The CFD simulations were performed using ANSYS CFX, solving for the compressible flow equations using the $k-\omega$ SST turbulence model. A low-Re approach for the modelling of the boundary layer was employed. The mesh is unstructured and consists primarily of tetrahedral elements with prismatic elements on regions containing boundary layers. The computational domain is divided into an interior cylindrical sector containing one box-blade and an outer quasi-2D domain, see Figure 10. The interior domain is set as rotating, and the two domains are connected through frozen rotor interfaces. The mesh size is 29-40 million cells, depending on calculation case. Grid and domain convergence has been demonstrated for each type of case[1].

Coefficients of thrust and propeller efficiency for different advance ratios J are presented in Figure 11 and Figure 12 respectively. As can be seen, there is good agreement between measured experimental data and CFD results at low speed. At advance ratios approaching 0.92 the CFD shows a lower level of thrust. Part of this difference was found to be due to pressure differences in the rig hub. The CFD thrust values increased and approached the experimental data to within 10% at J=0.92 when the nacelle upstream geometry was modeled in more detail (not shown).

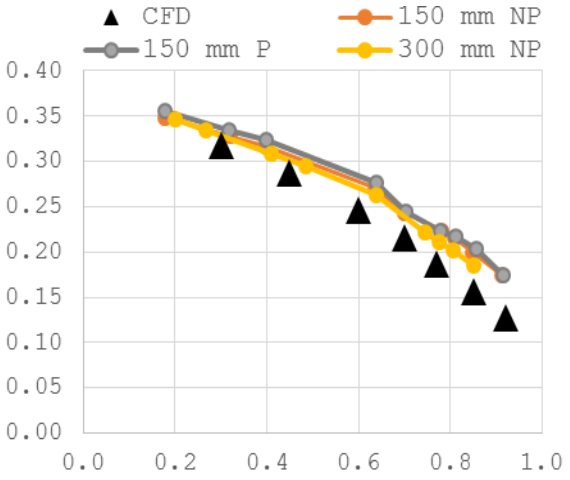

Figure 11 - Coefficients of thrust as function of advance ratio. Cases: CFD 150 mm, Non-Polished 150 mm (NP), Polished 150 mm (P), and non-polished 300 mm (NP).

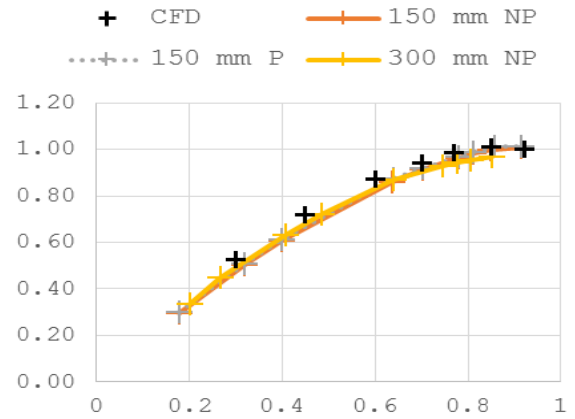

Figure 12 - Normalized propeller efficiency as function of advance ratio. CFD, non-polished 150 mm (NP), polished 150 mm (P), and non-polished 300 mm (NP).

Figure 13 shows the typical flow for the GPX313 in a constant radius cylindrical cross section. Leading (LB) and trailing (TB) blades refer to the direction of rotation. The high Mach number zone on the suction side of the leading (right) blade does not extend to the trailing (left) blade, indicating that interference effects are weak at low flight speed.

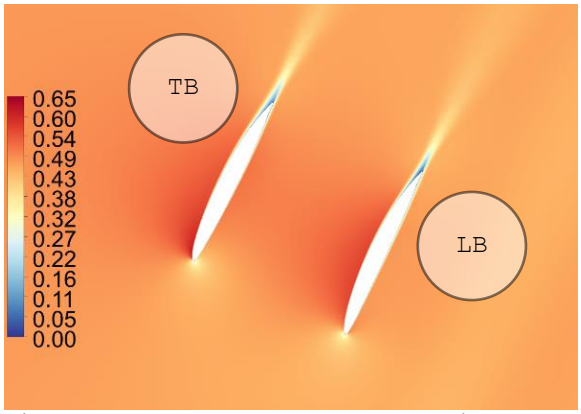

Figure 13 - GPX313: J=0.77, tip speed 204 m/s. Mach number plot at r/R = 75%. Due to selection of coordinate system for the analysis this figure is mirror imaged relative to e.g. Figure 8.

High-speed conditions

The operating point for high-speed conditions is chosen as typical for a future passenger aircraft with open rotor engines, being Mach 0.75 and an altitude of 10 668 m. A propeller diameter of 0.75 m was chosen as a compromise to avoid low Reynolds number effects while limiting the computational expense.

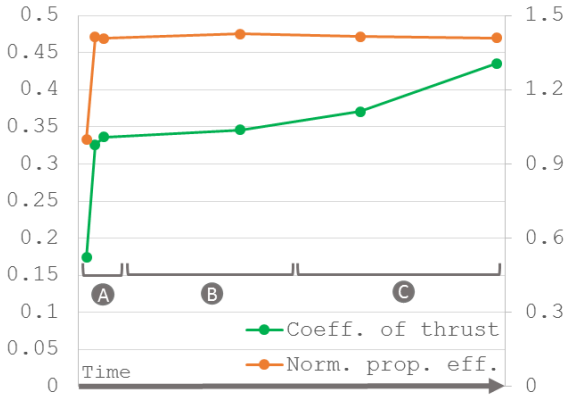

Figure 14 - The development of thrust (left axis) and efficiency relative to the first design (right) over time.

The understanding of how the box-propeller works has been increasing over time, and new measures to increase performance have been developed, see Figure 14. The improved thrust and efficiency are mainly due to better adaptation of the Boxprop blade tip to the propeller streamtube (A), changing

pitch angle and blade passage spacing (B), and the use of different pitch angle and camber distributions for each blade half (C). The distributions have to be tailored to the flow that is induced by both blade halves simultaneously, and to decrease the blade interference.
The first interference phenomenon affecting blade performance is the effect of the induced flow from the trailing blade (TB) on the incidence on the leading blade (LB). For equal LB and TB blade angles, the LB will experience a lower incidence, leading to less loading and thrust on that blade section. To increase LB thrust, one can increase its blade angle.

The second interference effect is the low pressure region that forms in the passage between the blade halves. This low pressure region decreases the pressure on the TB pressure side, leading to lower thrust on that blade half. If the passage area decreases aggressively, choking might occur. For better performance, the blade angle of the LB can be increased, its camber decreased, or blade spacing increased. These measures will lead to less low pressure on the TB pressure side, since these changes alleviate the flow contraction.

Table 1 - GPX701 characteristics.	
Number of blades	5
Diameter [m]	0.75
HTR	0.4
Activity factor	1784
J	3.54
Freestream Mach	0.75
N [rpm]	4997
Airfoil	NACA 16
C_T	0.451

One preliminary attempt at alleviating the effects of the blade interference is the GPX701, see Table 1. The activity factor of the GPX701 is chosen equal to that of the SR-7L propeller from the Large-Scale Advanced Prop-Fan (LAP) research program.

The interference effects near the hub were reduced through increasing the blade angle of the LB and decreasing its camber. This is visible in Figure 15, and this setup produced similar loading on both blade halves (122 N/m on the LB and 147 N/m on the TB).

The interference effects become more pronounced closer to the blade tip. The Mach number distribution at 75% radius is shown in Figure 16. In comparison with the low speed case shown in Figure 13, a region of high Mach number in the blade passage is visible, corresponding to a low pressure area that extends towards the pressure side of the TB. As was mentioned before, this decreases the thrust on the TB, but increases that of the LB. The sectional loading for the LB is 284 N/m and 176 N/m for the TB. At this radius the passage is supersonic across the entire passage, and a relatively weak shock extends along its rear.

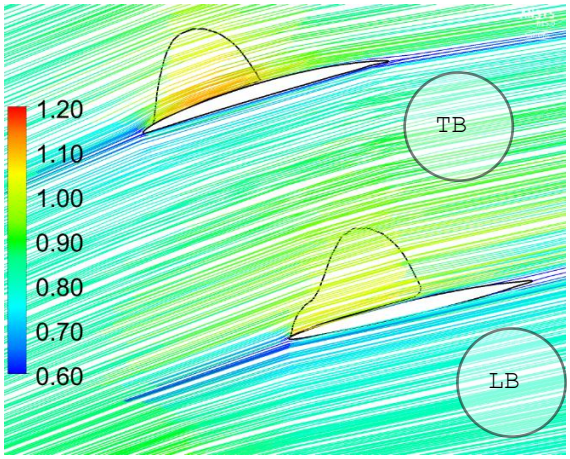

Figure 15 - GPX701, streamline plot at r/R = 50%. Mach number along streamlines. Sonic line is shown black. Mirror imaged, see caption of Figure 13.

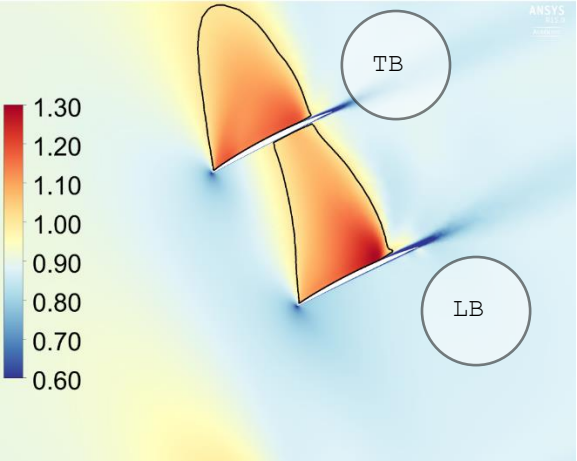

Figure 16 - GPX701: Mach number plot at r/R = 75%. The black lines denote a sonic Mach number. Mirror imaged, see caption for Figure 13.

Wake analysis method

A wake analysis method was derived and applied on a conventional propeller rotor. The method relates the energy changes in particles that travel through the propeller, and enables a breakdown of these energies into enthalpy, kinetic, and turbulent kinetic energy.

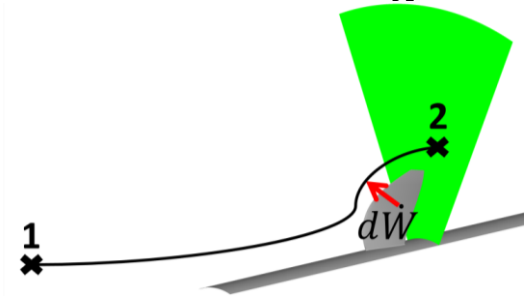

Figure 17 - Illustration of work added to a fluid element flowing from a point far upstream (1) to a point downstream of the propeller (2). Plane of integration marked green.

Consider an elemental fluid particle flowing through a turbomachine, see Figure 17. In a coordinate system rotating with the propeller, the flow will be steady. However, the velocities will be defined in reference to a stationary frame. The work added to the particle between a point upstream of the propeller and a control point downstream of the rotor lying on a plane, can be calculated from the total enthalpy change Δh_0, as specified in Eq. (1) ~~(1)~~ ~~(1)~~.

$$d\dot{W} = \Delta h_0 d\dot{m} = \Delta h_0 \rho_2 u_n dA \tag{1}$$

In the following steps it is assumed that the wake is evaluated in planes normal to the axial direction, for which the normal velocity u_n becomes the axial velocity. Integrating the particle work over a plane behind the propeller yields the shaft power:

$$P_{shaft} = \int_A d\dot{W} = \int_A \Delta h_0 \rho_2 u_n dA \tag{2}$$

The total enthalpy change can be expanded into its constituents:

$$\Delta h_0 = \Delta\left(h + \frac{1}{2}u_i u_i + k\right) \tag{3}$$

The kinetic energy can be further expanded into its components, in their cylindrical form:

$$\frac{1}{2}u_i u_i = \frac{1}{2}(u_x^2 + u_r^2 + u_\theta^2) \tag{4}$$

In order to capture the structure of the wake and tip vortex, the velocities $u_i(r,\theta)$ can be divided into an *axisymmetric velocity* $U_i(r)$ (circumferentially averaged, density weighted) and an associated *perturbation* $v_i(r,\theta)$*:*

$$u_i(r,\theta) = U_i(r) + v_i(r,\theta) \tag{6}$$

$$U_i = \frac{1}{\kappa}\int_0^{2\pi} \rho_2 u_i d\theta \qquad \kappa = \int_0^{2\pi} \rho_2 u_n d\theta \tag{7}$$

To illustrate the utility of this analysis, a conventional blade inspired by the SR-7L propeller was designed and simulated at the same cruise conditions as the GPX701 and using similar methodology as the cases mentioned previously in this paper. The main difference is the use of a hexahedral mesh. As expected, the tip vortex and the blade wake dominate the perturbation velocities shown in Figure 18.

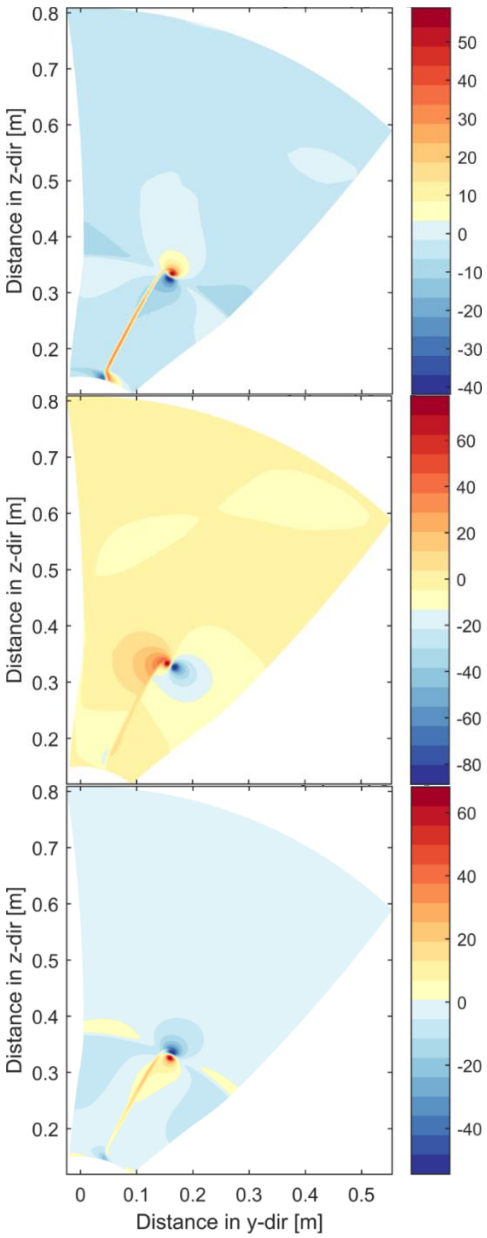

Figure 18 - Perturbation velocity fields. From the top: streamwise, radial and tangential velocity [m/s].

The plane is located half a blade height downstream of the propeller blade. The main usefulness of this method will be the ability to quantify different types of loss terms in propeller wakes, which will allow a more detailed comparison of the Boxprop and a conventional propeller. The perturbation is also the source of interaction noise for a rear counter rotating propeller.

Conclusions

This work has been successful in explaining and quantifying the remaining uncertainties between the numerical flow analysis and experimental results obtained from previous work in the static test rig.
Significant deformation causing untwist, propeller roughness and nacelle boundary layer ingestion have been shown to cause a majority of the thrust and torque differences observed.
The CFD results show good agreement with the first wind tunnel tests performed on the GPX313, with the remaining difference only somewhat larger than the measurement uncertainty.

Future Boxprop test campaigns will involve propellers manufactured from materials with higher specific stiffness and strength. It was concluded from a pre-study that a milled propeller from aircraft grade aluminum will meet the rig safety requirements and achieve surface smoothness required for fully smooth flow without any after treatment process. The AM alternatives SLM and EBM are also of great interest but appropriate polishing methods must be incorporated before the surface smoothness will be good enough for these small-scale propellers.

Acknowledgements

This work has been partially financed by the Swedish National Aeronautical Research Program (NFFP), which is jointly run by the Swedish Armed Forces, Swedish Defence Materiel Administration and the Swedish Governmental Agency for Innovation Systems. This work was partially funded by Chalmers University of Technology in Gothenburg, Sweden. The experimental work was carried out at the Division of Fluid Dynamics, Department of Applied Mechanics at

Chalmers University under the auspices of Dr Valery Chernoray and Professor Tomas Grönstedt. The authors would also like to thank the ambitious thesis workers Sandra Busch and Isak Jonsson that have performed the analysis and testing described in this article. Moreover, we would like to recognize the work of the Chalmers student project team that provided valuable insights regarding the manufacturing methods and materials for future high-speed propeller testing[11].

References

[1] Avellán, R. and Lundbladh, A., "Boxprop, a forward-swept joined-blade propeller", 21st ISABE Conference, June 9 – 13, 2013, Busan, Korea, ISABE-2013-1108.

[2] Avellán, R. and Lundbladh, A., "Air Propeller Arrangement and Aircraft", International application published under the patent cooperation treaty,WO2011/081577 A1, 2011.

[3] Bowles, M. D., 2010, "The Apollo of Aeronautics – NASA's Aircraft Energy Efficiency Program 1973-1987", NASA SP-2009-574, NASA HQ, Washington DC.

[4] Van Zante, D. E., 2015, "PROGRESS IN OPEN ROTOR RESEARCH: A U.S. PERSPECTIVE", GT2015-42203, Proceedings of ASME Turbo Expo 2015, June 15-19, 2015, Montreal, Canada.

[5] Gubisch, M., 2014, "SNECMA plans 2019 Open-Rotor Flights" Air Transport, Flight International 14-20 January 2014.

[6] Mankins, J. C., 1995, "Technology Readiness Levels – a white paper", NASA Advanced Concepts Office, June 6th 1995.

[7] Simonsen, E., 2007, "When the Hercules took the air", Boeing Frontiers, Vol. VI, Iss. VII, p.6-7, Nov. 2007.

[8] Kretschmann, D. E., 2010, "Mechanical Properties of Wood". In: Ross, R. J. ed., "Wood Handbook – Wood as an Engineering Material", General Technical Report FPL-GTR-190. Madison, WI: U.S. Chapter 5, pp.1-46.

[9] ASTM D2555-06(2011), "Standard Practice for Establishing Clear Wood Strength Valuyes", ASTM International, West Conshohocken, PA, 2011.

[10] Oxford Performance Materials, 2015, "OXFAB® Technology", OPM, Rev 2015April06.

[11] Alphonce, F., Bjelanovic, M., Hellåker, A., Huezo-Martinez, M., Lahoni, A., Wachter, E., Wadenvik, W., 2014, "The box-bladed Propeller – Development of a Wind Tunnel Prototype", Chalmers Student Project Report, Chalmers University of Technology, Gothenburg.

[12] Microtek finishing, 2012, "MMP Technology",http://www.microtekfinishing.com/microtek_mmp.php,(accessed June 25 2015).

[13] Cheema M. S. et al, 2012, "Development in abrasive flow machining: a review on experimental investigations using abrasive flow machining variants and media", Proc. of the Inst. Of Mech. Eng. Part B: Journal of Engineering Manufacture, 226(12), pp. 1951-1962.

[14] Flack, K. A. and Schultz, M. P., 2010, "Review of Hydraulics Roughness Scales in the Fully Rough Regime", Journal of Fluids Engineering, ASME J. Fluids Eng. 2010:132(4):0411203-041203-10.

[15] Schlichting, H., 1979, "Boundary-Layer Theory", 7th edition, McGraw-Hill, New York, USA.

[16] Olofsson, J. and Pettersson, V., 2013, "Experimental Investigation of an Innvoative High-speed Propeller", Master's Thesis Report, Chalmers University of Technology, Gothenburg, Sweden, 2013.

[17] Violette, J.A., Sullivan, W.E., Turnberg, J.E., 1984, "Large-Scale Advanced Prop-Fan (LAP) blade design", NASA-CR-174790, Hamilton Standard, Windsor Locks, CT, United States.